Available online at www.sciencedirect.com
SCIENCE DIRECT®
Journal of Organometallic Chemistry 690 (2005) 3937–3945
Journal of Organometallic Chemistry
www.elsevier.com/locate/jorganchem

Synthesis, structure, catalytic transfer hydrogenation and biological activity of cyclometallated ruthenium(III)2-(arylazo)phenolate complexes

G. Venkatachalam [a], R. Ramesh [a,*], S.M. Mobin [b]

[a] *School of Chemistry, Bharathidasan University, Tiruchirappalli 620 024, India*
[b] *National Single Crystal X-ray Diffraction Facility, IIT Bombay, Mumbai 400 076, India*

Received 12 April 2005; received in revised form 13 May 2005; accepted 24 May 2005
Available online 5 July 2005

Abstract

A series of mononuclear organoruthenium complexes of the type $[RuX(PPh_3)_2(L)]$ (X = Cl or Br; L = 2-(arylazo)phenolate ligand) have been synthesized from the reaction of five 2-(arylazo)phenol ligands with ruthenium(III) precursors, viz. $[RuCl_3(PPh_3)_3]$ and $[RuBr_3(PPh_3)_2(CH_3OH)]$ in benzene under reflux. In all these reactions, the 2-(arylazo)phenolate ligand replaces one triphenylphosphine molecule, two chlorides or bromides and one methanol from the precursors leading to five-membered cyclometallated species. The 2-(arylazo)phenol ligands behave as dianionic tridentate C, N, O donors and coordinated to ruthenium by dissociation of the phenolic proton and the phenyl proton at the *ortho* position of the phenyl ring. The compositions of the complexes have been established by elemental analysis, magnetic susceptibility measurement, FT-IR, UV–Vis and EPR spectral data. These complexes are paramagnetic and shows intense d–d and charge transfer transitions in chloroform. The solution EPR spectrum of the complex **7** in dichloromethane at 77 K shows rhombic distortion around the ruthenium ion. The structural conformation of the complex **1** has been carried out by X-ray crystallography. The redox behavior of the complexes has been investigated by cyclic voltammetry and the potentials are observed with respect to the electronic nature of substituents (R) in the 2-(arylazo) phenolate ligands. These complexes catalyze transfer hydrogenation of benzophenone to benzhydrol with up to 99.5% in the presence of *i*-prOH/KOH. Further, these complexes have shown great promise in inhibiting the growth of both Gram +ve and Gram −ve bacteria, viz. *Staphylococcus aureus NCIM 2079* and *Escherichia coli NCIM 2065* and fungus *Candida albicans NCIM 3102*.

Keywords: Ruthenium(III); Cyclometallation; Crystal structure; Electrochemistry; Catalytic transfer hydrogenation; Biological activity

1. Introduction

The cyclometallation reaction, i.e., the intramolecular activation of aromatic C–H bonds of coordinated ligands by transition metals has been widely studied [1–5]. Conventionally cyclometallation has involved one ligating group holding a metal center close to C–H bond and subsequent closure of the ring via the formation of carbon to metal bond [6,7]. Since the first cyclometallated complex was synthesized, cyclometallation has become an important part of organometallic chemistry. More recently, transition metal catalyzed transfer hydrogenation reaction using isopropanol as a hydrogen source, has become an efficient method in organic synthesis [8]. Noyori et al. [9–11] discovered a ruthenium(II) complexes in the presence of a base and isopropanol, proved to be excellent catalysts for the transfer hydrogenation of ketones under mild conditions. Further, a large number of transition metal phosphine complexes have been used as catalysts in transfer hydrogenation

* Corresponding author. Tel.: +91 431 240 7053; fax: +0091 431 240 7045/2407020.
E-mail address: ramesh_bdu@yahoo.com (R. Ramesh).

0022-328X/$ - see front matter © 2005 Elsevier B.V. All rights reserved.
doi:10.1016/j.jorganchem.2005.05.039

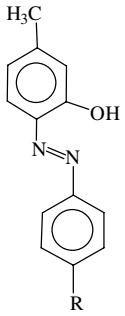

Where, R = Cl : HL1
CH_3 : HL2
OCH_3 : HL3
OC_2H_5 : HL4
H : HL5

Fig. 1. 2-(Arylazo)phenol ligands.

of aldehydes [12] or ketones [13] due to characteristic steric and electronic properties of tertiaryphosphine ligands [14]. In addition, the N, N and O, N donors of the ligands play an important role in catalytic reactions. Though a number of cyclometallated ruthenium(II) [4,15] and rhodium(III) [16] complexes are known, no reports are available on synthesis and catalytic transfer hydrogenation of cyclometallated ruthenium(III)2-(arylazo)phenolate complexes containing triphenylphosphine and chlorides/bromides. Chen et al. [17] have proposed that intercalation, hydrogen bonding and π–π interaction are some of the features implicated in the mode of action of ruthenium complexes as antitumour and antimetastatic agents. Further more, the presence of ruthenium–halogen bonds in several ruthenium complexes exhibiting anticancer activity suggesting that these bonds may also play some important role [18].

We describe here the synthesis of 10 cyclometallated ruthenium(III) complexes containing 2-(arylazo)phenol ligands, chloride or bromide and triphenylphosphine. The molecular and electronic structures of the trivalent complexes are probed with the help of X-ray crystal structure, in combination with FT-IR, electronic and EPR spectra. The relative stabilities of oxidation and reduction states are monitored electrochemically. Further, the catalytic activity towards transfer hydrogenation of benzophenone and biological activity against certain human pathogenic bacteria and fungus of these complexes are reported. The following 2-(arylazo)phenol ligands (Fig. 1) were used to synthesis the mononuclear ruthenium(III) complexes.

2. Experimental

2.1. Materials and physical measurements

All the reagents used were chemically pure and AR grade. Solvents were purified and dried according to standard procedures [19]. $RuCl_3 \cdot 3H_2O$ was purchased from Loba Chemie Pvt. Ltd., and was used without further purification. The primary amines were purchased from Aldrich.

The analysis of carbon, hydrogen and nitrogen were performed in Carlo-Erba 1106-model 240 Perkin Elmer analyzer at Central Drug Research Institute (CDRI), Lucknow, India. FT-IR spectra were recorded in KBr Pellets with a JASCO 400 plus spectrophotometer. A CARY 300 Bio UV–Vis Varian spectrophotometer was used to record the electronic spectra. Room temperature solid-state magnetic susceptibilities were measured by using EG and G model 155 vibrating sample magnetometer at SAIC, Chennai. EPR spectra were recorded on JEOL JES-FA200 EPR spectrometer at X-band frequencies for powder sample at room temperature and solution at 77 K. Electrochemical measurements were made using a Princeton EG and G-PARC model potentiostat using a glassy carbon working electrode and all the potentials were referenced to Ag/AgCl electrode. The catalytic yields were determined using HP 6890 series GC-FID with a DP-5 column of 30 m length, 0.32 mm diameter and 0.25 μm film thickness. The antimicrobial screening studies were carried out at Periyar College of Pharmaceutical Sciences, Tiruchirappalli, India and the bacteria, fungus were obtained from National Chemical Laboratory, Pune, India. The ruthenium(III) precursor complexes $[RuCl_3(PPh_3)_3]$ [20] and $[RuBr_3(PPh_3)_2(CH_3OH)]$ [21] were prepared according to the literature reports. The 2-(arylazo)phenol ligands were prepared by coupling diazotized aniline and *p*-substituted anilines with *p*-cresol [19].

2.2. Synthesis of ruthenium(III) complexes

All the reactions were carried out under strictly anhydrous conditions. The ruthenium(III) precursors $[RuCl_3(PPh_3)_3]$ [0.15 mmol; 0.150 g] (or) $[RuBr_3(PPh_3)_2(CH_3OH)]$ [0.15 mmol; 0.135 g] and 2-(arylazo)phenol ligands (HL1–HL5) (0.15 mmol; 0.031–0.038 g) were taken in 20 ml benzene. The mixture was heated under reflux for 2 h until a deep green solution was obtained and the reactions were monitored by thin-layer chromatography. The solvent was then evaporated under reduced pressure, which was subjected to purification by silica gel column chromatography. On elution with chloroform, the green band was collected. The ruthenium complexes were obtained as crystalline solid of yield 70% upon complete evaporation of the solvent. The elemental (CHN) analysis is consistent with the composition proposed for all the complexes (Table 1). IR and electronic spectral data of all the complexes are summarized in Table 2.

2.3. Procedure for catalytic transfer hydrogenation of benzophenone

Under inert atmosphere a mixture containing benzophenone (1.25 mmol; 0.227 g), the ruthenium catalyst (0.0125 mmol) and 0.0625 mmol of KOH was heated to reflux in 10 ml of *i*-prOH for 2 h. The catalyst was re-

Table 1
Analytical data of ruthenium(III)2-(arylazo)phenolate complexes

Complexes	Colour	Found (Calc.) %		
		C	H	N
$[RuCl(PPh_3)_2(L1)]$ (**1**)	Green	64.76(64.92)	4.86(4.30)	2.88(3.09)
$[RuBr(PPh_3)_2(L1)]$ (**2**)	Green	61.53(61.88)	4.42(4.10)	2.72(2.94)
$[RuCl(PPh_3)_2(L2)]$ (**3**)	Green	67.98(67.77)	4.23(4.74)	3.03(3.16)
$[RuBr(PPh_3)_2(L2)]$ (**4**)	Green	64.32(64.53)	4.99(4.51)	2.81(3.01)
$[RuCl(PPh_3)_2(L3)]$ (**5**)	Green	66.28(66.57)	5.06(4.66)	2.88(3.10)
$[RuBr(PPh_3)_2(L3)]$ (**6**)	Green	63.58(63.44)	4.73(4.44)	2.73(2.96)
$[RuCl(PPh_3)_2(L4)]$ (**7**)	Green	67.04(66.86)	4.46(4.46)	2.98(3.05)
$[RuBr(PPh_3)_2(L4)]$ (**8**)	Green	63.23(63.76)	4.65(4.58)	2.67(2.91)
$[RuCl(PPh_3)_2(L5)]$ (**9**)	Green	67.66(67.56)	4.18(4.37)	3.08(3.21)
$[RuBr(PPh_3)_2(L5)]$ (**10**)	Green	64.45(64.28)	4.87(4.59)	2.83(3.06)

Table 2
IR and electronic spectral data of the ruthenium(III)2-(arylazo)phenolate complexes

Complexes	IR frequencies (cm^{-1})		λ_{max} (nm) ε (dm^3/mol/cm)
	ν_{C-O}	$\nu_{N=N}$	
1	1301	1373	655(756)[b] 423(1356)[a] 364(2700) 273(6528)
2	1305	1388	652(848)[b] 416(2248)[a] 322(4660) 276(7712) 256(8212)
3	1303	1384	656(1500)[b] 421(2580)[a] 334(5460) 318(6340) 273(12,013)
4	1299	1376	653(1728)[b] 414(3408)[a] 352(5548) 315(7536) 275(12,969)
5	1288	1380	637(1948)[b] 422(2736)[a] 359(6272) 317(7432) 281(12,404)
6	1312	1374	631(1580)[b] 421(2870)[a] 361(5092) 276(10,116)
7	1297	1380	634(1128)[b] 425(1564)[a] 359(3440) 318(4050) 273(8172)
8	1310	1384	631(1172)[b] 418(2044)[a] 361(3824) 272(8320)
9	1301	1388	658(1404)[b] 417(2312)[a] 331(5576) 316(6608) 282(11,584)
10	1311	1379	658(1072)[b] 413(2340)[a] 334(4252) 255(8744)

[a] Charge transfer transition.
[b] d–d transition.

moved from the reaction mixture by the addition of diethylether followed by filtration and subsequent neutralization with 1 M HCl. The ether layer was filtered through a short path of silica gel by column chromatography. The filtrate was subjected to GC analysis and the hydrogenated product benzhydrol was identified and determined with authentic sample in all the cases.

2.4. Antimicrobial assays

The in vitro antimicrobial screenings of free ligands and their ruthenium(III) complexes were tested for their effect on certain human pathogenic bacteria and fungus by disc diffusion method. The ligands and the ruthenium complexes were stored dry at room temperature and dissolved in 10% DMSO in methanol. Both the Gram +ve (*Staphylococcus aureus NCIM 2079*) and Gram −ve (*Escherichia coli NCIM 2065*) bacteria were grown in nutrient agar medium and incubated at 37 °C for 48 h followed by frequent subculture to fresh medium and were used as test bacteria. *Candida albicans NCIM 3102* grown as sabourard Dextrose Agar medium were incubated at 27 °C for 72 h followed by periodic sub culturing to fresh medium and were used as test fungus. Then the petriplates were inoculated with a loop full of bacterial and fungal culture and spread throughout the petriplates uniformly with a sterile glass spreader. To each disc the test samples and reference antibiotic (tetracycline 10 μg/clotrimazole 10 μg) were added with a sterile micropipette. The plates were then incubated at 35 ± 2 °C for 24–48 h and at 27 ± 1 °C for bacteria and fungus, respectively. Plates with disc containing respective solvents served as control. Inhibition was recorded by measuring the diameter of the inhibitory zone after the period of incubation. Triplicates were maintained and the experiment was repeated thrice and the average values are presented.

2.5. X-ray crystallography

Single crystals suitable for X-ray diffraction were grown from mixture of chloroform–acetonitrile solution at room temperature. A crystal of approximate size $0.25 \times 0.25 \times 0.15$ mm was mounted on a glass fiber with epoxy cement mounted on a Nonius MACH 3 Diffractometer equipped with graphite monochromatic Mo Kα radiation (0.71073 Å). Unit cell dimensions were obtained using 25 centered reflections in θ range 5.1100–

11.9900. The intensity data were collected by ω–2θ scan mode, and corrected by Lorentz polarization and absorption effects using psi-scan (ψ-scan). Three standard reflections monitored after every 200 reflections and three intensity control reflections monitored every hour, and showed no significant changes (<3%). The structure was solved by direct methods SHELXS97 and refined by full-matrix least squares against F^2 using SHELXL97 software [22,23]. Non-hydrogen atoms were refined with anisotropy thermal parameters. All hydrogen atoms were geometrically fixed and allowed to refine using a riding model.

3. Results and discussion

A series of low spin cyclometallated organoruthenium complexes of the type $[RuX(PPh_3)_2(L)]$ (X = Cl or Br; L = 2-(arylazo)phenolate ligands) were synthesized in good yields from the reaction of $[RuCl_3(PPh_3)_3]$ and $[RuBr_3(PPh_3)_2(CH_3OH)]$ with 2-(arylazo)phenol ligands (HL1–HL5) in dry benzene in equal molar ratio (Scheme 1). It has been observed that arylazo ligands replace two chlorides or bromides, one PPh_3 and CH_3OH group and the oxidation state of ruthenium remains unchanged during the formation of cyclometallated species. All the complexes are found to be air stable in both the solid and liquid state at room temperature, non-hygroscopic in nature. The synthesized ruthenium complexes are highly soluble in common solvents such as chloroform, dichloromethane, toluene and benzene producing intense green solutions.

3.1. Spectral characterization

Infrared spectra of the complexes show many sharp and strong vibrations within 1600–400 cm^{-1} and the assignment of all these vibrations has not been attempted. However, the ligands exhibit bands around 1429–1439 and 1270–1278 cm^{-1} corresponding to –N=N– and phenolic C–O, respectively. On complexation –N=N– appears at 1373–1388 cm^{-1} and this red shifting supports the coordination of azo-N to the metal center [24,25]. The coordination through phenolic oxygen is confirmed by the increase of C–O at higher frequencies in the region 1288–1304 cm^{-1} in all the complexes. This was further supported by the disappearance of ν_{OH} band in the range 3450–3439 cm^{-1} in all the complexes. In addition, these complexes show new bands near 540, 690, 740 and 1556 cm^{-1} which are due to PPh_3 ligand.

Electronic spectra of all the complexes have been recorded in chloroform solution in the range 200–800 nm. The representative spectrum of the complex **1** is shown in Fig. 2. All the complexes display 4–5 intense absorptions in the region 658–255 nm. The intense absorption in the visible region at 658–631 nm is due to d–d transitions and the absorption at 425–413 nm is probably due to ligand to metal charge transfer transitions. The spectral profiles below 400 nm are very similar which are due to π–π* and n–π* ligand centered transitions taking place in the coordinate 2-(arylazo)phenol ligands. Such spectral behavior has been observed in similar octahedral ruthenium(III) complexes [16,26].

The room temperature magnetic susceptibility measurements show that these complexes (**1**: 1.90 BM, **5**: 1.94 BM, **8**: 1.87 BM) are one electron paramagnetic, which supports the trivalent state of ruthenium (low spin d^5; $S = 1/2$) in an octahedral environment. The solid state EPR spectra of all the complexes were recorded in X-band frequencies at room temperature. All the complexes exhibit well-defined single isotropic features near $g_{iso} = 2.00$ (complexes **1**–**10**: $g_{iso} = 2.02$ to 2.06). Such isotropic lines are usually the results of either intermolecular spin exchange, which can broaden the lines or occupancy of the unpaired electron in a degenerate orbital. However, the EPR spectrum of the complex **7** recorded in dichloromethane solution at 77 K shows

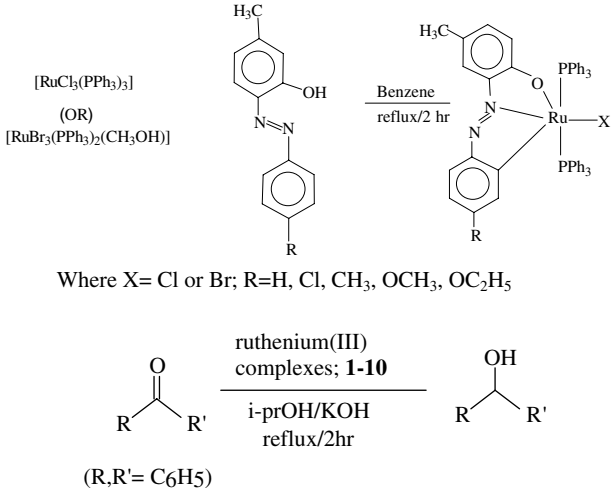

Scheme 1.

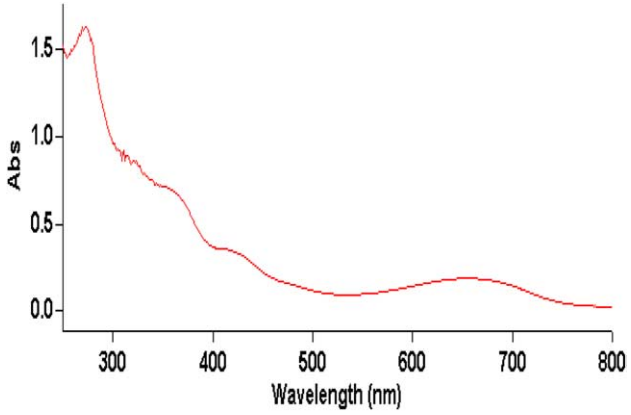

Fig. 2. Electronic spectra of complex **1** in dichloromethane.

rhombic spectrum (Fig. 3) with three distinct '*g*' values ($g_x \neq g_y \neq g_z$: $g_x = 2.203$, $g_y = 2.092$, $g_z = 1.956$). The rhombicity of the spectra reflects the asymmetry of electronic environments around ruthenium in these complexes [27].

3.2. Crystal structure

The summary of single crystal X-ray structure refinement results is shown in Table 3 and selected bond length and bond angles are presented in Table 4. To understand the coordination mode of 2-(arylazo)phenolate ligands and stereochemistry of ruthenium(III) complexes, the X-ray crystal structure of a representative complex **1** has been determined and the ORTEP view of this complex is shown in Fig. 4. The 2-(arylazo)phenolate ligands act in a tridentate fashion, binding the metal center at O(1), N(1), C(1) forming two five-membered chelate rings with bite angles of 77.93(12) (O(1)–Ru–N(1)) and 75.61(14) (C(1)–Ru–N(1)). The entire tridentate ligand skeleton together with ruthenium and chloride constitute the equatorial plane while the chloride is in transposition with respect to azo nitrogen. The two PPh_3 ligands occupy mutually *trans* to each other, the Ru(1)–P(1) 2.406(12) and Ru(1)–P(2) 2.400(12) bond distances are equal from the metal center. The overall $CNOP_2Cl$ coordination sphere around ruthenium is distorted octahedral in nature, which is reflected in all the bond parameters around ruthenium. As all the complexes display similar spectral and electrochemical properties, the other nine complexes are assumed to have similar structure to that of complex **1.**

3.3. Electrochemistry

The electrochemical properties of all the complexes have been examined cyclic voltammetrically under N_2 atmosphere at glassy carbon working electrode in chloroform (0.05 M:NBu_4ClO_4) and the redox potentials are expressed with reference to Ag/AgCl. Cyclic voltammogram of all the complexes (1×10^{-3}M) display a quasi-reversible oxidation (Ru^{IV}/Ru^{III}) and quasi-reversible reduction (Ru^{III}/Ru^{II}) peaks at the scan rate of 100 mV s^{-1}. The potentials are summarized in Table 5

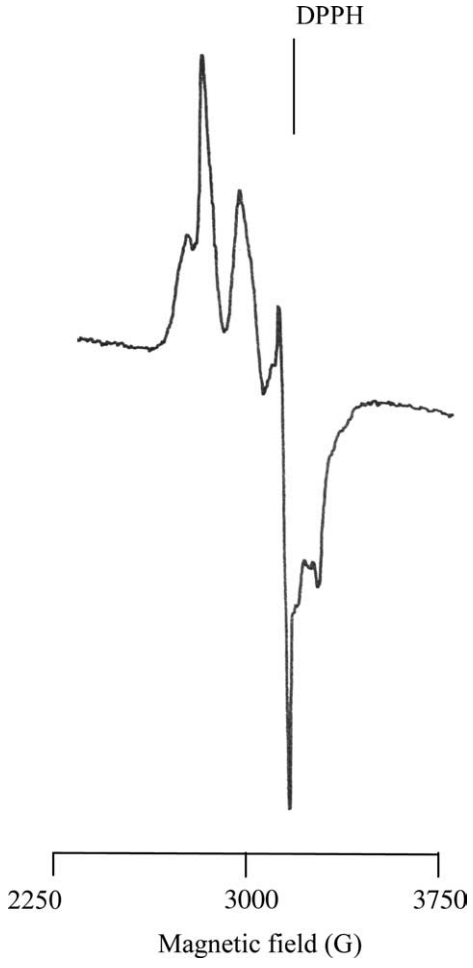

Fig. 3. EPR spectrum of the complex **7** in dichloromethane solution at 77 K.

Table 3
Crystal data and structure refinement for complex **1**

Identification code	bdu01a
Empirical formula	$C_{49}H_{39}Cl_2N_2OP_2Ru$
Formula weight	905.73
Temperature (K)	293(2)
Wavelength (Å)	0.71073
Crystal system, space group	Monoclinic, $P2_1/n$
Unit cell dimensions	
a (Å)	12.2790(12)
b (Å)	19.0410(16)
c (Å)	19.140(3)
α (°)	90
β (°)	107.843(12)
γ (°)	90
Volume (Å^3)	4259.8(9)
Z, calculated density (Mg/m^3)	4, 1.412
Absorption coefficient (mm^{-1})	0.608
F(0 0 0)	1852
Crystal size (mm)	$0.25 \times 0.25 \times 0.15$
Theta range for data collection (°)	1.54–24.93
Index ranges	$0 \leqslant h \leqslant 14$, $0 \leqslant k \leqslant 22$, $-22 \leqslant l \leqslant 21$
Reflections collected/unique	7830/7460 [$R_{int} = 0.0335$]
Completeness to $2\theta = 24.93$	96.4%
Absorption correction	Psi-scan
Maximum and minimum transmission	0.9143 and 0.8628
Refinement method	Full-matrix least-squares on F^2
Data/restraints/parameters	7460/0/515
Goodness-of-fit on F^2	0.954
Final R indices [$I > 2\sigma(I)$]	$R_1 = 0.0422$, $wR_2 = 0.0798$
R indices (all data)	$R_1 = 0.1085$, $wR_2 = 0.0959$
Largest difference peak and hole (e A^{-3})	0.327 and −0.319

Table 4
Selected bond lengths (Å) and bond angles (°) of complex **1**

Bond lengths (Å)		Bond angles (°)	
Ru–C(1)	2.022(4)	P(1)–Ru–P(2)	174.56(4)
Ru–N(1)	2.010(3)	N(1)–Ru–Cl(1)	178.32(10)
Ru–O(1)	2.120(3)	C(1)–Ru–N(1)	75.61(14)
Ru–P(1)	2.4064(12)	N(1)–Ru–O(1)	77.93(12)
Ru–P(2)	2.4001(12)	C(1)–Ru–O(1)	153.43(14)
Ru–Cl(1)	2.3630(11)	C(1)–Ru–Cl(1)	103.54(12)
C(9)–C(10)	1.514(6)	O(1)–Ru–Cl(1)	102.97(8)
N(1)–N(2)	1.292(4)	N(1)–Ru–P(1)	95.72(10)
O(1)–C(13)	1.317(5)	C(1)–Ru–P(1)	91.40(12)
N(1)–C(7)	1.402(5)	O(1)–Ru–P(1)	88.73(9)
N(2)–C(6)	1.399(5)	Cl(1)–Ru–P(1)	85.74(4)
		Cl(1)–Ru–P(2)	88.83(4)
		N(1)–Ru–P(2)	89.71(10)
		C(1)–Ru–P(2)	89.57(12)
		O(1)–Ru–P(2)	92.79(9)

ESD in parentheses.

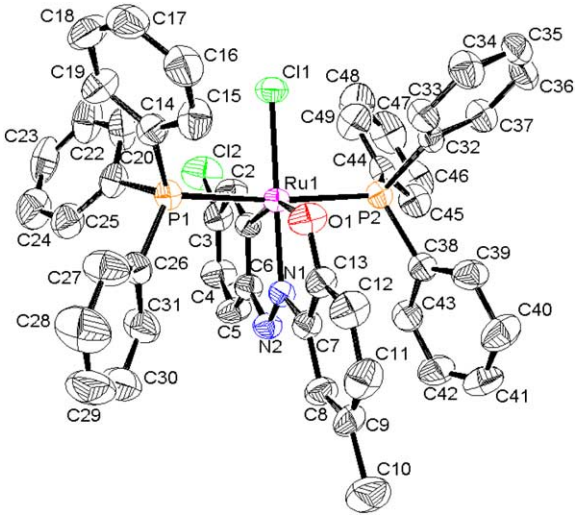

Fig. 4. The ORTEP diagram of the complex $[RuCl(PPh_3)_2(L1)]$ (**1**).

and a representative voltammogram is shown in Fig. 5. All the complexes showed well-defined waves $E_{1/2}$ lies at +0.67 to + 0.86 V (Ru^{IV}/Ru^{III}) and −0.60 to −0.43 V (Ru^{III}/Ru^{II}). These redox processes are quasi-reversible with large peak-to-peak separation (ΔE_p) of 100–240 mV [28], and the current height measurement reveals one electron redox processes. These redox potentials ($E_{1/2}$) are independent of the various scan rates, supporting quasi-reversibility. The couples at more positive and less negative potentials are believed to corresponding metal oxidation (Eq. (1)) and metal reduction (Eq. (2)), respectively.

$$[Ru^{III}(PPh_3)_2(L)(X)] \rightleftharpoons [Ru^{IV}(PPh_3)_2(L)(X)]^+ + e^- \quad (1)$$

$$[Ru^{III}(PPh_3)_2(L)(X)] + e^- \rightleftharpoons [Ru^{II}(PPh_3)_2(L)(X)]^- \quad (2)$$

The redox potentials shift to lower values upon alkyl substitution and the amount of shift is ~0.17 and ~0.13 V for oxidation and reduction, respectively. The potentials of both the oxidation (Ru^{IV}/Ru^{III}) and reduction (Ru^{III}/Ru^{II}) have been found to be sensitive to the nature of the substituent (R) in the 2-(arylazo)phenolate ligands. The formal potentials $E_{1/2}$ increases with increase in electron withdrawing nature of the substituent (R). The plot of $E_{1/2}$ vs. σ (σ – Hammet constant of R: $OCH_3 = -0.27$, $OC_2H_5 = -0.24$, $CH_3 = -0.17$, $H = 0.00$, $Cl = 0.23$) [29] is linear for both couples (Fig. 6) with slopes of 0.37 V (Ru^{III}/Ru^{IV}) and 0.32 V (Ru^{III}/Ru^{II}) for complexes **1**, **3**, **5**, **7**, **9** and 0.39 V (Ru^{III}/Ru^{IV}) and 0.27 V (Ru^{III}/Ru^{II}) corresponds to complexes **2**, **4**, **6**, **8** and **10**. This linear correlation of the redox potentials of the electronic nature (σ) of the substituents clearly shows that a single substituent on the 2-(arylazo)phenolate ligand, which is four bonds away from the metal center, can influence the metal-centered potentials in a predictable manner. Further, oxidation and reduction potentials do not show any systematic variation with the change in chloride or bromide in the ruthenium complexes. Hence, from the electrochemical data it is clear that the present ligand system is ideally suitable for stabilizing the higher oxidation state of ruthenium ion and the electron transfer reactions take place without gross changes in the stereochemistry of the complexes [30].

Table 5
Electrochemical data of ruthenium(III)2-(arylazo)phenolate complexes

Complexes	Ru^{III}/Ru^{IV}				Ru^{III}/Ru^{II}			
	E_{pa} (V)	E_{pc} (V)	$E_{1/2}$ (V)	ΔE_p (mV)	E_{pa} (V)	E_{pc} (V)	$E_{1/2}$ (V)	ΔE_p (mV)
1	+0.92	+0.79	+0.86	130	−0.38	−0.48	−0.43	100
2	+0.93	+0.78	+0.86	140	−0.37	−0.55	−0.46	180
3	+0.84	+0.61	+0.72	230	−0.47	−0.69	−0.58	220
4	+0.80	+0.65	+0.72	150	−0.47	−0.63	−0.55	160
5	+0.78	+0.58	+0.68	200	−0.49	−0.68	−0.59	190
6	+0.73	+0.62	+0.67	110	−0.48	−0.72	−0.60	240
7	+0.74	+0.62	+0.69	120	−0.50	−0.64	−0.57	140
8	+0.75	+0.61	+0.68	140	−0.47	−0.63	−0.55	160
9	+0.91	+0.70	+0.80	210	−0.42	−0.58	−0.50	160
10	+0.92	+0.71	+0.81	210	−0.41	−0.53	−0.47	120

Supporting electrolyte: NBu_4ClO_4(0.005 M); Complex: 0.001 M; Solvent: $CHCl_3$; $\Delta E_p = E_{pa} - E_{pc}$, where E_{pa} and E_{pc} are anodic and cathodic potentials, respectively; $E_{1/2} = 0.5(E_{pa} + E_{pc})$; scan rate: 100 mV s^{-1}.

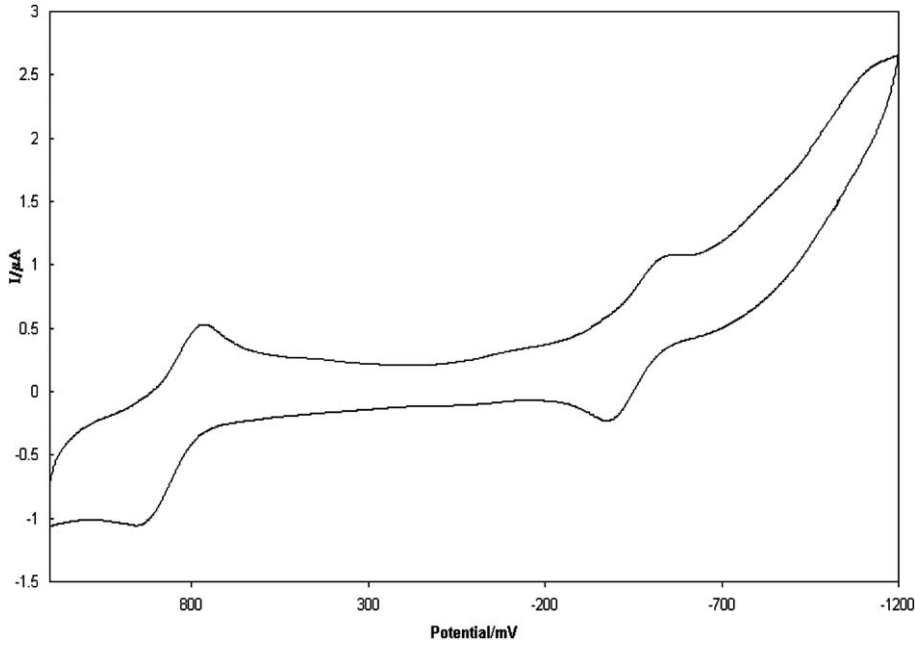

Fig. 5. Cyclic voltammogram of the complex **2** in chloroform solution (0.05 M TBAP) at the scan rate of 100 mV s^{-1}.

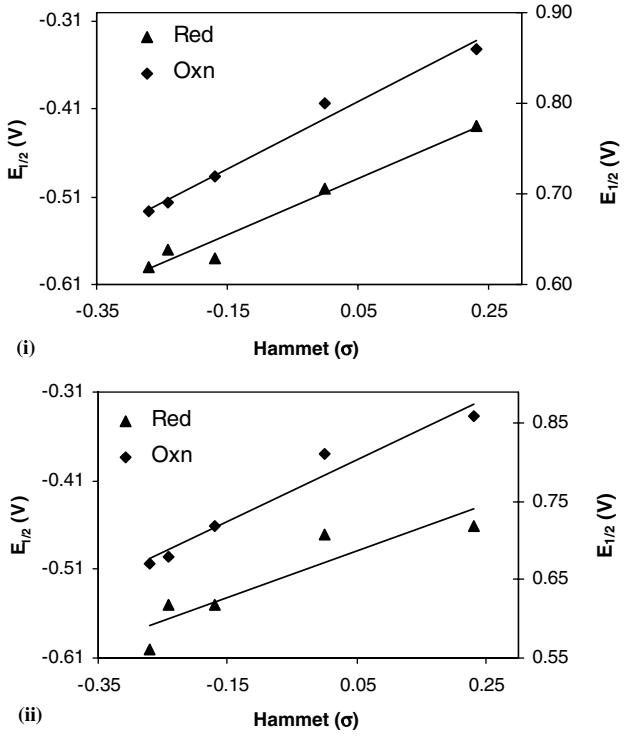

Fig. 6. Least-squares plot of (i) $E_{1/2}$ values oxidation (Ru^{IV}/Ru^{III}) and reduction (Ru^{III}/Ru^{II}) potentials of complexes **1**, **3**, **5**, **7**, **9** and (ii) $E_{1/2}$ values of oxidation (Ru^{IV}/Ru^{III}) and reduction (Ru^{III}/Ru^{II}) potentials of the complexes **2**, **4**, **6**, **8**, **10** vs σ.

3.4. Catalytic activity in transfer hydrogenation of ketones

The catalytic transfer hydrogenation of benzophenone by all the ruthenium(III) complexes was carried out in the presence of isopropanol/KOH (Scheme 1). All the complexes catalyze benzophenone to benzhydrol with high conversion. The benzhydrol formed after 2 h of reflux were determined by gas chromatography with authentic samples.

In this reaction, the base facilitates the formation of ruthenium alkoxide by abstracting the proton of the alcohol and subsequent β-elimination of alkoxide generates ruthenium-hydride, which is an active species in this reactions. This is the mechanism proposed by several workers on the studies of ruthenium complexes catalyzed transfer hydrogenation reaction by metal hydride intermediates [31]. Although no mechanistic studies have been performed, the catalytic transformation of benzophenone most probably follows the classical

Table 6
Catalytic activities in transfer hydrogenation of benzophenone by ruthenium(III) complexes/*i*-prOH-KOH[a]

Complexes	Product	Conversion (%)[b]
1	Benzhydrol	92.6
2	Benzhydrol	96.0
3	Benzhydrol	97.6
4	Benzhydrol	99.5
5	Benzhydrol	99.2
6	Benzhydrol	95.5
7	Benzhydrol	99.0
8	Benzhydrol	98.0
9	Benzhydrol	92.8
10	Benzhydrol	94.0

[a] Condition: reactions were carried out 82 °C using 1.25 mmol of benzophenone (10 ml isopropanol); Catalyst/Ketone/KOH ratio 1:100:2.5.
[b] Conversion of benzhydrol after 2 h, GC determined.

Table 7
Antimicrobial activity of ruthenium(III) 2-(arylazo) phenolate complexes

Complexes	Diameter of zone of inhibition (mm)					
	Stap. aureus NCIM 2079		*E. coli NCIM 2065*		*C. albicans NCIM 3102*	
	50 ppm	100 ppm	50 ppm	100 ppm	50 ppm	100 ppm
HL1	–	8	–	7	–	–
1	11	13	10	10	8	10
2	10	12	11	13	10	12
HL2	8	8	7	8	–	8
3	11	13	11	11	11	12
4	10	12	9	11	8	11
HL3	–	7	–	9	–	7
5	11	16	13	11	7	10
6	9	10	9	11	9	11
HL4	–	7	9	11	–	7
7	10	13	11	13	–	9
8	12	13	9	12	7	9
HL5	–	–	8	7	9	8
9	9	12	10	13	11	13
10	10	11	9	11	8	9
Standard	25	24	24	24	12	12

'–', no inhibition. Standard: Tetracycline (10 μg) for bacteria and clotrimazole (10 μg) for fungus. Solvent: DMSO (No inhibitory against the microorganisms).

pathway in which ketones coordinate to hydride-ruthenium metal intermediate. The formation of ruthenium(III) hydride active species as catalytic intermediate is proposed for this catalytic reactions. The observed effects seem to indicate that the hydride transfer from the metal to the coordinated ketones is the final step in the catalytic cycle. It has been observed that the catalytic activity varies with respect to substituent (R) in the azo fragment. The electron donating substituent present in the complexes found to be highly active in the catalytic reactions showing conversion of >96% (Table 6). Even though several catalytic system have been reported to support the transfer hydrogenation of ketones, complexes of this types are new for its saturated C, N, O donor environment of the ruthenium(III)2-(arylazo)phenolate complexes.

3.5. Antimicrobial activity

The in vitro cytotoxicity of ligands and their complexes were screened in order to evaluate the activity against the certain human pathogenic bacteria and fungus at two different concentrations and the results are shown in Table 7. The microbes used were both the Gram +ve (*S. aureus NCIM 2079*), Gram −ve (*E. coli NCIM 2065*) bacteria and the fungus *C. albicans*. The results indicate that the complexes exhibit considerable activity compared to their parent ligands against the same microbes under identical experimental conditions and the toxicity of ruthenium chelate increases on increasing the concentration. This would suggest that chelation could facilitate the ability of a complex to cross a cell membrane [32,33]. A possible mode of toxicity increase can be explained by Tweedy's Chelation theory [34]. Chelation considerably reduces the polarity of the metal ion because of partial sharing of its positive charge with donor groups and possible π-electron delocalization over the whole chelate ring. Such a chelation could enhance the lipophilic character of the central metal atom, which subsequently favors its permeation through the lipid layer of the cell membrane. In addition to this, azo nitrogen may be the active site and is capable of forming hydrogen bond with the cell constituents [35]. The results revealed that the nature of the substituents (R) on the phenyl ring was found either to increase or decrease the biological activity of the complexes and may be due to the variation of electron density on the azo-nitrogen. The observed results seem to conclude that the present ruthenium(III)2-(arylazo)phenolate complexes possess more cytotoxicity than the other metal complexes against the microbes *S. aureus*, *E. coli* [36,37] and *C. albicans* [38]. The variation in the effectiveness of different compounds against different organism depends either on the impermeability of the cells of microbes or the differences in ribosome of microbial cells.

4. Conclusion

The present work describes a simple and convenient route to synthesize of a series of cyclometallated ruthenium(III)2-(arylazo)phenolate complexes incorporating triphenylphosphine and chloride/bromide ligands. The X-crystal structure of the complex reveals a distorted octahedral environment around ruthenium. All the complexes were found to be efficient catalyst in transfer hydrogenation of benzophenone to benzhydrol and the

conversion is up to 99.5%. Further, the possible explanations for the mode of action of these complexes against different microbes are described.

Acknowledgments

The authors express their sincere thanks to Council of Scientific and Industrial Research (CSIR), New Delhi [Grant No. 01 (1725)/02/EMR-II] for financial support. One of the authors G.V. thanks CSIR for the award of Senior Research Fellowship (SRF). We thank the National Single Crystal X-ray Diffraction Facility, IIT Bombay, Mumbai, for providing X-ray data collection and Prof. P. Sambasiva Rao, Pondicherry University to record EPR spectra.

Appendix A. Supplementary data

Crystallographic data for the structural analysis have been deposited with Cambridge crystallographic center, CCDC No. 256955. Copies of this information may be obtained free of charge from The Director, CCDC, 12 Union road, Cambridge.CB2 1EZ, UK (email: deposit@ccdc.cam.ac.uk). Supplementary data associated with this article can be found, in the online version at doi:10.1016/j.jorganchem.2005.05.039.

References

[1] I. Omae, Organometallic Intramolecular-coordination Compounds, Elsevier, Amsterdam, 1986.
[2] A.M. Clark, C.E.F. Rickard, W.R. Roper, L.J. Wright, J. Organomet. Chem. 598 (2000) 262.
[3] R. Ares, M. Lopez-Torres, A. Fernandez, M.J. Pereira, R.A. Saurez, R. Mosteiro, J.J. Fernandez, J.M. Vila, J. Organomet. Chem. 665 (2003) 87.
[4] R. Acharyya, F. Basuli, R.Z. Wang, T.C.W. Mak, S. Bhattacharya, Inorg. Chem. 43 (2004) 704.
[5] S. Nag, P. Gupta, R.J. Butcher, S. Bhattacharya, Inorg. Chem. 43 (2004) 4814.
[6] A.D. Ryabov, Chem. Rev. 90 (1990) 403.
[7] J.W. Slater, J.P. Rourkee, J. Organomet. Chem. 688 (2003) 112.
[8] J. Hannedouche, G.J. Clarkson, M. Wills, J. Am. Chem. Soc. 126 (2004) 986.
[9] M. Kitamura, M. Yoshimura, N. Kanda, R. Noyori, Tetrahedron 55 (1999) 8769.
[10] M. Yamakawa, H. Ito, R. Noyori, J. Am. Chem. Soc. 122 (2000) 1466.
[11] R. Noyori, T. Ohkuma, Angew Chem. Int. Ed. 40 (2000) 40.
[12] K.I. Na, S. Huh, K.M. Sung, M.-J. Jun, Polyhedron 15 (1996) 1841.
[13] M. Ito, M. Hirakawa, K. Nurata, T. Ikariya, Organometallics 20 (2001) 379.
[14] (a) C.A. Mc Auliffe, W. Levason, Phosphine, Arsine and Stilbene Complexes of the Transition Elements, Elsevier, Amsterdam, 1979;
(b) D.W. Meek, L.H. Pignolet (Eds.), Homogenous Catalysis with Metal Phosphine Complexes, Plenum Press, New York, 1983.
[15] W.I. Cross, K.R. Flower, R.G. Pritchard, J. Organomet. Chem. 601 (2000) 164.
[16] S. Dutta, S.M. Peng, S. Bhattacharya, J. Chem. Soc., Dalton Trans. (2000) 4623.
[17] H. Chen, J.A. Parkinson, S. Parsons, R.A. Coxall, R.O. Gould, P.J. Sadler, J. Am. Chem. Soc. 124 (2002) 3064.
[18] P.M.T. Piggot, L.A. Hall, A.J.P. White, D.J. Williams, Inorg. Chim. Acta 357 (2004) 207.
[19] A.I. Vogel, Text Book of Practical Organic Chemistry, fifth ed., Longman, London, 1989.
[20] J. Chatt, G.J. Leigh, D.M.P. Mingos, R.J. Paske, J. Chem. Soc. A (1968) 2636.
[21] T.A. Stephenson, G. Wilkinson, J. Inorg. Nucl. Chem. 28 (1966) 954.
[22] G.M. Sheldrick, Acta Crystallogr., Sec. A 46 (1990) 467.
[23] G.M. Sheldrick, Program for Refinement of Crystal Structure, University of Gttingen, Germany, 1997.
[24] S. Goswami, R. Mukherjee, A. Chakravorty, Inorg. Chem. 22 (1983) 2825.
[25] B. Mondal, M.G. Walwalker, G.K. Lahiri, J. Chem. Soc., Dalton Trans. (2000) 4209.
[26] P.K. Sinha, J. Chakravarty, S. Bhattacharya, Polyhedron 16 (1997) 81.
[27] N.C. Pramanik, S. Bhattacharya, Polyhedron 16 (1997) 3047.
[28] P. Byabartta, J. Dinda, P.K. Santra, C. Sinha, K. Pannerselvam, F.-L. Liao, T.H. Lu, J. Chem. Soc., Dalton Trans. (2001) 2825.
[29] L.P. Hammett, Physical Organic Chemistry, second ed., McGraw-Hill, New York, 1970.
[30] K. Sui, S.M. Peng, S. Bhattacharya, Polyhedron 19 (1999) 631.
[31] (a) K.J. Haack, S. Hashiguchi, A. Fujji, J. Takehera, T. Ikariya, R. Noyori, Angew. Chem., Int. Ed. Engl. 36 (1997) 285;
(b) J.-E. Backvall, J. Organomet. Chem. 652 (2002) 105.
[32] C.S. Allardyce, P.J. Dyson, D.J. Ellis, P.A. Salter, J. Organomet. Chem. 668 (2003) 35.
[33] R. Ramesh, S. Maheswaran, J. Inorg. Biochem. 96 (2003) 457.
[34] B.G. Tweedy, Phytopathology 55 (1964) 910.
[35] S. Chakraborty, A.K. Bera, S. Bhattacharya, S. Ghosh, A.K. Pal, S. Ghosh, A. Banerjee, J. Organomet. Chem. 645 (2002) 33.
[36] M. Joseph, V. Suni, M.R. Prathapachandra Kurup, M. Nethaji, A. Kishore, S.G. Bhat, Polyhedron 23 (2004) 3069.
[37] M. Nath, R. Jairath, G. Eng, X. Song, A. Kumar, J. Organomet. Chem. 690 (2005) 134.
[38] H.P.S. Chauhan, N.M. Shaik, J. Inorg. Biochem. 99 (2005) 538.